



Third-Generation Photovoltaic Cell Manufacturing Processes

Abdul Hai Alami , Shamma Alasad , Haya Aljaghoub ,
Mohamad Ayoub , Adnan Alashkar , Ayman Mdallal ,
and Ranem Hasan 

Abstract

Most of the manufacturing techniques mentioned in this chapter have been visited in the previous chapters of this book. However, they are presented here in more details and comprehensive description, making this chapter a self-contained reference.

1 Introduction

The conventional silicon manufacturing processes for photovoltaic wafer production are steeped in history. There is a limited margin for substantial improvement or enhancement that would either dramatically increase the yield or significantly reduce the production costs. On the other hand, thin-film and third-generation photovoltaics still have no standard, unanimously adopted manufacturing techniques. This leaves wide room for examining the best techniques that would maximize a figure-of-merit (FOM) that usually is the ratio between the produced power (or efficiency) and production cost of each cell. Another important aspect for second and third-generation PV is the amenability to

automation, or what is usually known roll-to-roll (R2R) production. The speed of which the PV cells are made, stitched together and prepared for dispatch largely and directly affect the FOM. And thus, the amenability of many of the available manufacturing processes discussed in this chapter to R2R manufacturing will be highlighted. The ease of use as well as capital investment are also important aspects to consider. This chapter will focus on technologies such as photolithography, spin coating, slot-die, and thermal evaporation as the most facile manufacturing technologies available on the market. Mastering these techniques requires time and experience to set all competing process parameters to values that produce the required response from the manufactured solar cells. The user should be prepared for a lot of material and consumable waste before the process could produce the desired outcomes.

2 Photolithography

Photolithography is a technique that is predominantly used to print surface contacts on silicon solar cells. The process is similar to ink-jet printing, where the ink sticks only to a predetermined design that is printed onto a substrate. In the case of semiconductor and solar cell device fabrication, the silicon wafer acts as the substrate, while the deposition, lithography, and etching process create the desired features (the ink). Given the optical exposure requirement to generate the pattern in semiconductor lithography, the process is referred to as “photolithography”. This process is extremely interesting as there exists a better access to 3D printers as well as cheap and advanced software to superpose the desired structure (e.g., front emitter contacts) on the silicon substrate. Figure 1 provides a schematic representation of the process steps.

To achieve a successful photolithographic feature, a series of steps need to be followed (Newport 2022). The process commences with substrate cleaning and preparation.

A. H. Alami (✉) · H. Aljaghoub · M. Ayoub · A. Mdallal ·
R. Hasan
University of Sharjah, Sharjah, United Arab Emirates
e-mail: aalalami@sharjah.ac.ae

H. Aljaghoub
e-mail: haljaghoub@sharjah.ac.ae

M. Ayoub
e-mail: mohamad.ayoub@sharjah.ac.ae

A. Mdallal
e-mail: ayman.mdallal@sharjah.ac.ae

S. Alasad · A. Alashkar
American University of Sharjah, Sharjah, United Arab Emirates
e-mail: g00070854@aus.edu

A. Alashkar
e-mail: b00028197@alumni.aus.edu

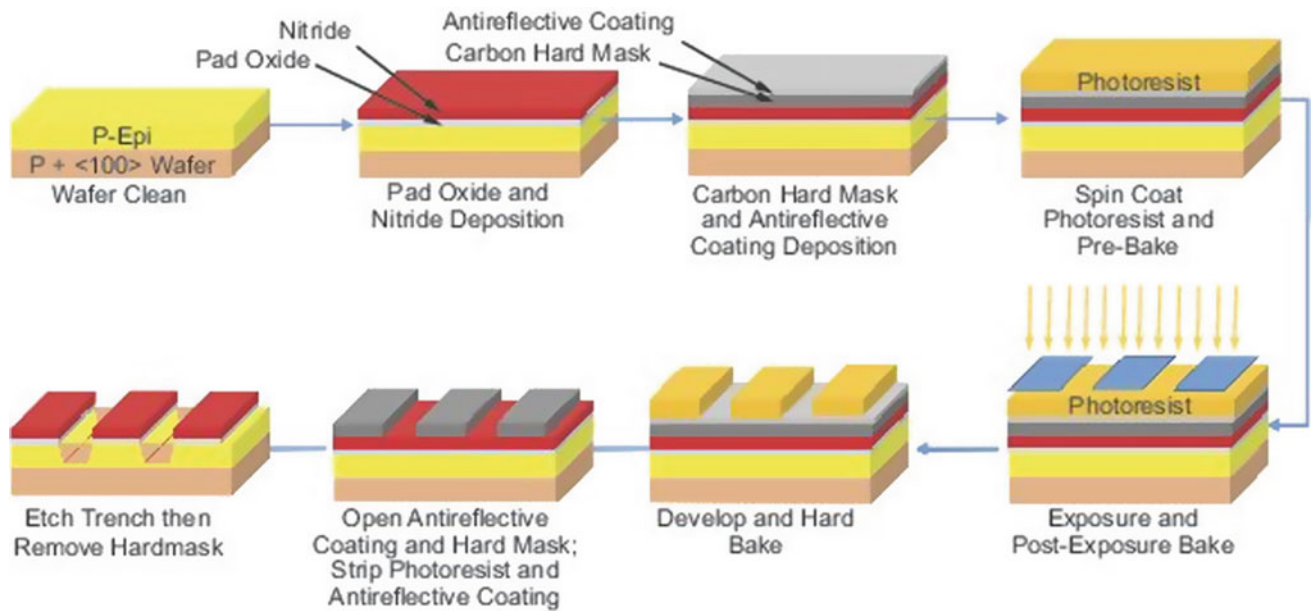


Fig. 1 Schematic representation of a semiconductor device patterning process (Newport 2022)

Next, layers of thermal oxide and silicon nitride are deposited on the substrate. This is followed by the inclusion of a carbon hard mask and an anti-reflective material. Subsequently, a layer of photoresist is then deposited, pre-baked, and aligned with the substrate, followed by an exposition to UV radiation and 4x 5x imaging. Post-exposure bake is then carried out to develop the pattern in the photoresist followed by a hard bake to remove any residue solvent. The dielectric anti-reflective coating (DARC) and hard mask pattern are opened through etching, and the photoresist as well as the DARC are removed. Trenches are then opened in the substrate through another separate etching process, and the hard mask is removed in the process. Finally, the surface is cleaned.

3 Screen Printing

Screen printing is a bulk coating process that is used in thin-film solar cells such as Cadmium-Telluride (CdTe), third-generation solar cells such as dye-sensitized solar cells and contact depositions in silicon based solar cells. Screen printing mainly consists of a frame around a silk-based screen and an either a metallic or a wooden squeegee. Figure 2 shows a depiction of the process, while Fig. 3 is an example of the process.

Other essential parts include a dye printed on a transparent sheet that is used to expose the desired coating shape on a UV-curable emulsion (a mold for the ink to follow while passing on the screen). The plastic-sheet-dye is placed beneath the uncured emulsion and above a UV-light source

for a substantial amount of time > 10 h. This step is crucial to ensure that the coated ink follows the targeted design.

1. Once the screen with a cured emulsion is prepared, it is placed on top of the to be coated substrate.
2. Then, the ink (deposited material) is placed on one end of the silk screen.
3. The screen is lifted at an angle with respect to the substrate.
4. Using the squeegee, the ink is spread to the other end of the silk screen to ensure that the entire emulsion is covered with ink.
5. The screen is placed back on top of the substrate.
6. Using the squeegee, and by applying sufficient pressure, the ink is pressed on the silk screen and passed onto the substrate.

Parameters that are important in the process of screen printing are the force applied by the squeegee (F), the speed of the squeegee (V_{sq}), the viscosity of the paste (η), the angle of the squeegee (α), and the print factor ($f(Q)$) shown in Eq. 1 (Hussain et al. 2022).

$$F[N] = \eta [N.s/m^2] V_{sq} [m/s] \frac{2\alpha [^\circ] \sin \alpha}{\alpha^2 - \sin^2 \alpha} f(Q) \quad (1)$$

3.1 Screen Printing—CdTe Thin-Film Solar Cells

In terms of thin-film CdTe solar cells, screen printing is mainly used to deposit the CdTe p type layer and the n-type

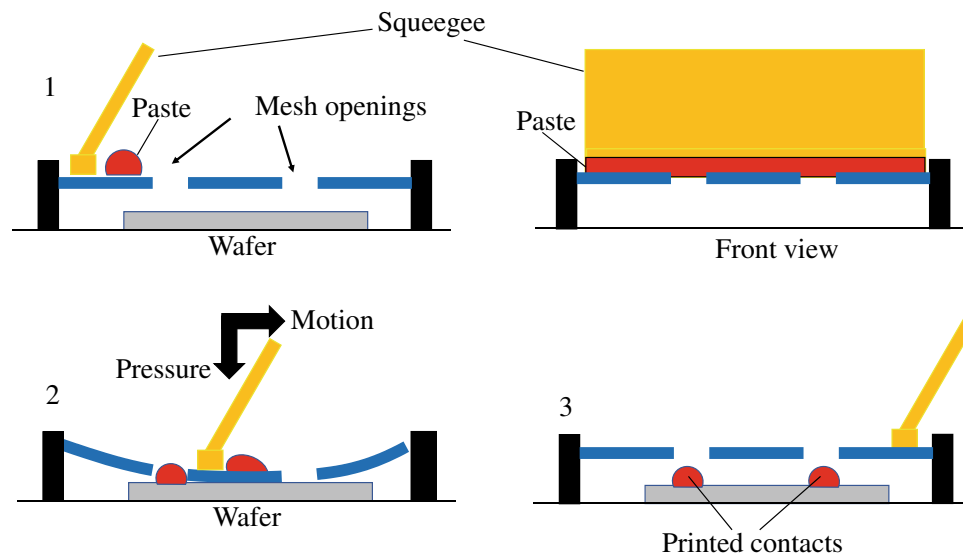


Fig. 2 Depiction of the screen-printing process steps



Fig. 3 Example of the screen-printing process (Hussain et al. 2022) (with permission 5273590576001)

CdS layer. However, the grain size based totally on these two materials through screen printing is very limited. Which is why the principle of sinters was introduced to these materials which consists of Cadmium chloride ($\text{CdCl}_2 \sim 1$ wt%) with an essential function that will help with the properties of the end film.

The sinter flux sticks to the host material (CdTe (5N) or CdS) in solid form. When the film is printed and goes through a heating post-treatment, the sinter flux melts and joins together the rather spread host materials grains and forms a film with larger grain size (up to $10 \mu\text{m}$ (<https://www.semanticscholar.org/paper/Thin-film-solar-cells-by-screen-printing-technology-Burgelman/f7a356e1c66f443a5604c07d69dbfc0de714cc77>) relative to the initial formation of it.

These screen-printing-inks are a combination of CdTe/CdS along with the previously mentioned sinters and a propanediol-based binder.

1. Respective inks are placed on the silk screen in the form of either CdTe or CdS particles along with CdCl_2 sinter flux.
 - a. The CdCl_2 sinter flux is chosen based on the solubility of both CdTe and CdS in it at moderate temperatures ($500\text{--}600^\circ\text{C}$), such as shown in Fig. 4.
2. The ink is printed on the screen and forms a film with small but dense grains.
3. The film is then heated to 600°C which melts the sinter flux and “sinters” the grains together forming large-grain-films of CdTe and CdS.
4. At 600°C , the vapor pressure reached by the CdCl_2 is sufficient to evaporate this volatile component leaving behind the desired materials on the substrate.

The process for screen-printing and sintering the CdTe/ CdCl_2 -based ink is showcased in Fig. 5.

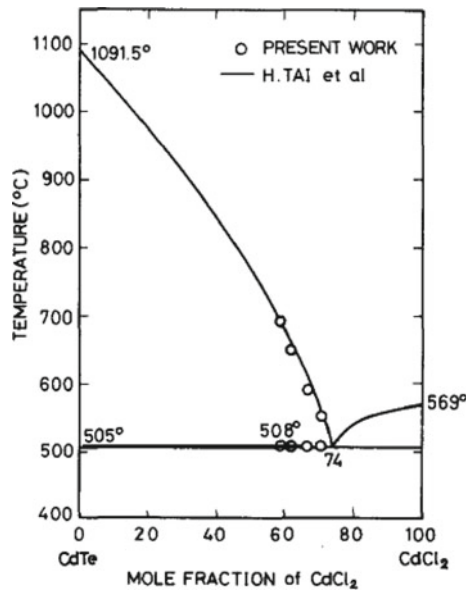


Fig. 4 CdTe–CdCl₂ phase diagram (Saraie et al. 1978)

3.2 Screen Printing—Silicon Solar Cells Contacts

Screen printing is used to achieve low-cost deposition of electrical contacts on silicon based solar cells. The material

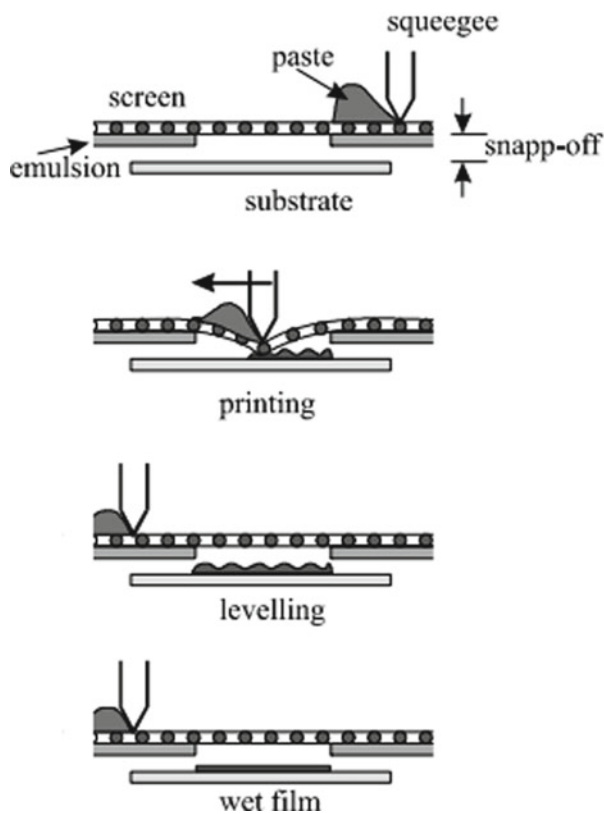


Fig. 5 Screen printing with subsequent sintering process (Burgelman 1998)

of choice is silver paste due to its excellent electrical properties. The silver paste is a mixture of silver powder (providing conductive electrical properties) and glass frits (lead borosilicate-based) (Guo et al. 2011), which scratch the silicon cell's surface and allow the silver powder to segregate at a desired depth in the silicon substrate. Organic solvents are also used to provide fluidity to the paste for the ease of screen printing.

- Following the standard procedure for screen printing, shown in Fig. 2, the silver paste is printed using a cured emulsion that is based on the design and shape of the contact fingers. With some conditions that define the design of the emulsion such as
 - The opening of the reticule must be larger than the largest particle contained in the paste.
 - To form the front contact, the emulsion is formed in a mesh shape with typically 325 wires per inch and a wire diameter of 30 μm .
- After the printing is done, the cells are dried at a temperature using an IR furnace that would allow the evaporation of the organic solvent component in the silver paste.
- A firing step is carried using a time varying temperature profile (500–900 °C) to form the front contacts in their final form.

4. During the firing step, the glass frits act as a sinter that allows a larger growth of the silver contacts. Achieving the same purpose as that by CdC_2 in CdTe-based thin-film cells.
5. The glass frit is also able to etch through deposited layers on the silicon substrate such as anti-reflective coating and passivating layers.

3.3 Screen Printing—Dye-Sensitized Solar Cells

Screen printing can be used to deposit essential layers in dye-sensitized solar cells such as a silver grid, for parallel type metal grid embedded DSSCs which is the closest we got in scaling up this type of solar cells as shown in Fig. 6, and the TiO_2 active layer.

1. A silver grid is deposited on an FTO surface and then dried at around $200\text{ }^\circ\text{C}$.
 - a. This layer enhances the conductivity of the cell by decreasing the sheet resistance to about $0.2\ \Omega/\text{cm}$.
2. The TiO_2 active material is screen printed using the previously mentioned screen-printing procedure.
 - a. The printed film is then dried and heated up to $500\text{ }^\circ\text{C}$ to activate the sintering process.
 - b. The dried TiO_2 film is then immersed in a dye solution ruthenium (II) in absolute ethanol ($\sim 70\%$) for $>$ day (Ramasamy et al. 2007).
 - c. The counter electrode which consists of platinum and an acidic solvent is screen printed and then sintered accordingly at $400\text{ }^\circ\text{C}$.



Fig. 6 Screen printed metal-grid embedded DSSC (Ramasamy et al. 2007) (With permission 5274140611103)

4 Spin Coating

Spin coating is a technique used to uniformly spread thin films of polymers, organic materials (Orava et al. 2014), or metal oxide inks (Solution Processed Metal Oxide Thin Films and for Electronic Applications 2020), on substrates such as glass, FTO, and flexible plastics. It utilizes the centrifugal force applied on a solution to spread it homogeneously over the selected substrate. Spin coating is also used in the microelectronics industry (Summers 2013), and it is at the forefront of the third-generation solar cells scene. In this section, the general spin coating system components, coating steps and principles, the advantages and disadvantages, as well as the application of spin coating in perovskite solar cells will be discussed.

4.1 System Components

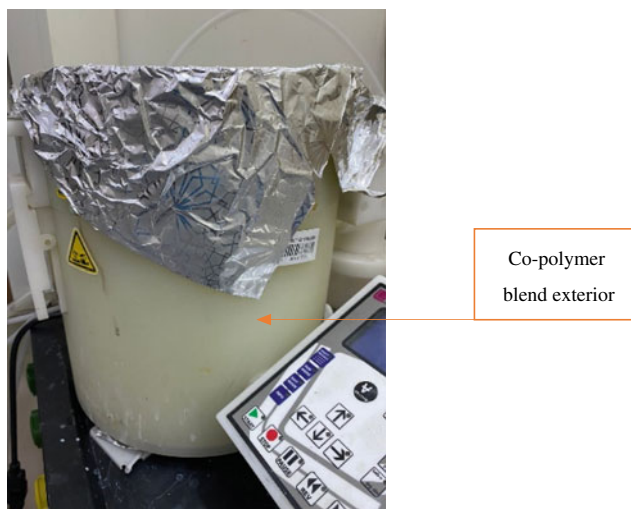
The heart of the spin coating machine is the rotating platform, the size (diameter), and rotational velocity of which determines the system capability. The motor selection is also important as it determines the torque applied on the platform and hence the ultimate rotational speeds. Although the process is extremely easy to use and many people have chosen to make the device themselves (check youtube.com for many examples), it is considered one of the most material intensive processes as the splash from the rotational motion of the solution before it solidifies is significant.

4.1.1 Device Hub

A specifically designed sturdy exterior is used to harbor the electrical and mechanical components that allow a spin coater to operate steadily under high rotational speed conditions, and it should also be of high tolerance toward solvents that are used in thin-film precursors. The exterior can be made of steel (<https://www.ossila.com/products/spin-coater>), natural polypropylene, which is a thermoplastic that offers good physical and chemical properties (<https://www.boedeker.com/Product/Polypropylene-Natural>), high chemical resistant PTFE that is stable in corrosive media (<http://www.standard-ptfe.com/chemical-resistance-guide-of-ptfe-and-filled-ptfe.php>, <https://www.spincoating.com/en/spin-coater-models/spincoater-polos300-advanced-spin-coating-machine/28/>), or solid co-polymer blends that achieve desired physical, mechanical, and chemical properties (<http://www.laurell.com/spin-coater/?model=WS-650-23B&s=2>), such as shown in Fig. 7, etc.

4.1.2 Motor

A spin coater motor provides the required torque to indirectly rotate the substrate, usually glass or FTO, along with



Co-polymer
blend exterior

Fig. 7 Spin coater exterior

the solution/precursor dispensed on it at desired speeds, reaching up to 12,000 rpm in some models (<https://www.spincoating.com/en/spin-coater-models/spincoater-polos300-advanced-spin-coating-machine/28/>, <http://www.laurell.com/spin-coater/?model=WS-650-23B&s=2>). In a DIY project, according to Teixeira et al. (2020), something as simple as the motor that is used to lift up or lower down windows of a car has sufficient torque (~ 12 N.m) to achieve speeds of 5000 rpm, which is suitable for some applications such as the coating of electron/hole transport layers used in third-generation solar cells.

Fig. 8 Vacuum-assisted substrate holder—side and top view



4.1.3 Substrate Holder

The substrate holder is the component that is directly being rotated by the motor of the spin coater. There are two main designs that are used in today's market:

- Vacuum-assisted circular turntable: Where the substrate is placed on a hollowed circular surface with an O-ring gasket, such as shown in Fig. 8, that aids with holding down the sample using the vacuum achieved between this surface and the substrate via an external vacuum-pumping system connected to the spin coater, such as shown in Fig. 9.
- Cavity Chuck: Alternatively, in some spin coater designs, the substrate is placed in a cut out cavity, also known as a chuck. The chuck boundaries are used to hold down the substrate in place without the need of a vacuum-pumping system, such as shown in Fig. 10.

4.1.4 Cover

Spin coaters utilize covers made of tempered glass or the same material as the device hub/interior, such as shown in Fig. 11. The cover is used to prevent the flinging of the precursor outside the spin coater boundaries while coating at high speeds, which is used as a safety measure and to avoid contamination of adjacent lab equipment.

4.1.5 Interface

Spin coaters are equipped with an integrated operating system that is accessible through an attached interface, shown in



Fig. 9 Spin coater vacuum system-nitrogen tank—compressor

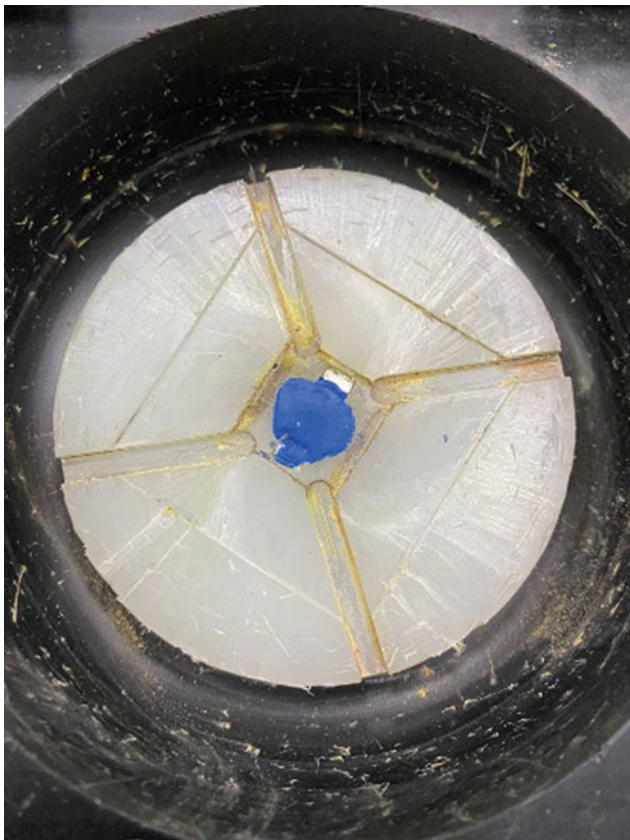


Fig. 10 Chuck substrate holder

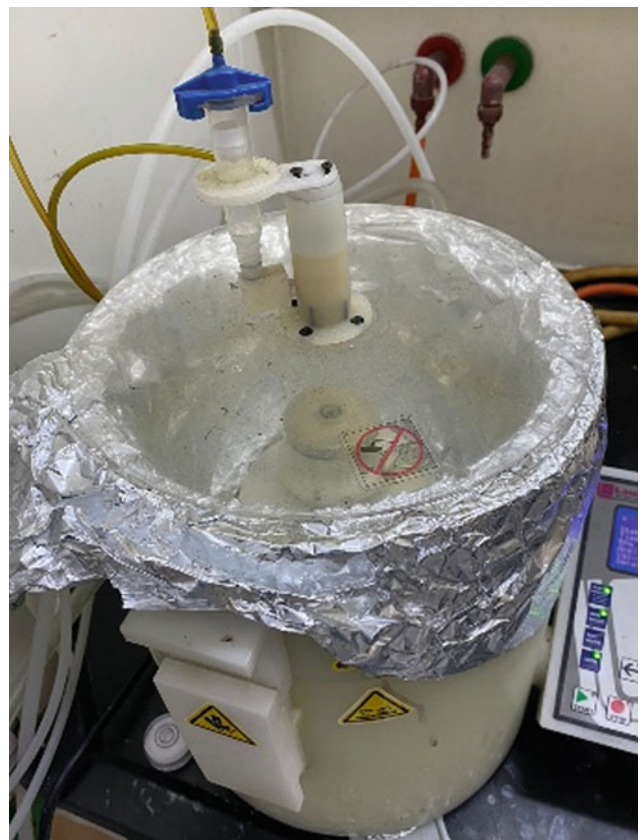


Fig. 11 Spin coater cover



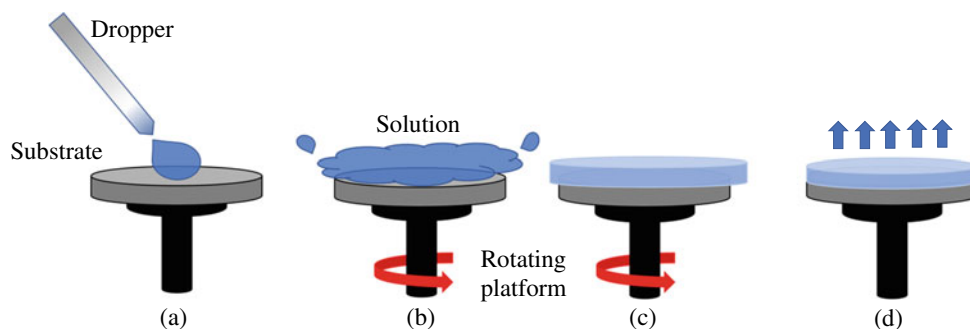
Fig. 12 Spin coater interface

Fig. 12. Through this interface, parameters such as rotational speed, time, stepping up speed, as well as multi-step programs can be input by the user according to their experiment's requirements.

4.2 Coating Steps and Principle

A spin coating process can be subdivided into 5 steps, which are pre-deposition, deposition, spinning up, spinning off, and evaporation (<https://www.ossila.com/pages/spin-coating>) such as shown in Fig. 13.

Fig. 13 Spin coating process steps **a** deposition, **b** spin up, **c** spin off, and **d** evaporation (Yilbas et al. 2019) (with permission: 5260980863854)



1. Pre-deposition

In some cases, substrates need to be UV treated to increase the wettability of the surface. Otherwise, the precursor would not stick to it and consequently ruin the end-film result.

2. Deposition

The precursor is dispensed onto the substrate using a pipette, and this can be done while the substrate is stationary (static spin coating), or it can be done while the substrate is rotating (dynamic spin coating) (<https://www.ossila.com/pages/spin-coating>). Dynamic spin coating is preferred over static spin coating in situations where the solvent's evaporation temperature is very low. Going through the dynamic route gives the solvent less time to evaporate uncontrollably in comparison with static spin coating, which leads to more reproducible results.

3. Spinning up

Centrifugal force spreads the dispensed precursor radially outwards, which results in covering the whole surface of the substrate (Mishra et al. 2019).

4. Spinning off

At this stage, the viscous force along with surface tension is dominating. This causes the excess precursor to be flung off the substrate, resulting in an even and level film across it (Mishra et al. 2019).

5. Evaporation

High volatile components (components that can evaporate at room temperature) are spontaneously evaporated at this stage, leaving behind the dry desired film. In some cases, such as the coating of the perovskite active layer in third-generation perovskite solar cells, the evaporation

process is aided with anti-solvents, such as chlorobenzene. Anti-solvents are dispensed during the coating process, and they result in better thin-film results by increasing the solvents evaporation rate (Yilbas et al. 2019).

The end-film thickness of a spin coating process can be estimated by Eq. (2), that is, based on the Emslie, Bonner and Peck model (Eq. 3).

$$h = \frac{h_0}{\sqrt{\left(1 + \frac{4\rho\omega^2 h_0^2 t}{3\eta}\right)}} \quad (2)$$

where

h_0 : thickness of the film at $t = 0$ (beginning of the coating process).

ρ : density of the fluid layer.

ω : rotational speed.

η : viscosity of the fluid layer.

t : time.

Similarly, the Emslie, Bonner, and Peck Model can be shown as follows:

$$\frac{\delta h}{\delta t} + \frac{\rho\omega^2 r}{\eta} h^2 \frac{\delta h}{\delta r} = -\frac{2\rho\omega^2 h^3}{3\eta} \quad (3)$$

where

$\frac{\delta h}{\delta t}$: rate of change in thickness.

$\frac{\delta h}{\delta r}$: rate of spreading.

However, with no regard to the evaporation of the solvents, the thickness obtained from this equation/model is not accurate.

a. Advantages and Disadvantages of Spin Coating

Advantages

- (i) Has the ability to achieve uniform thin films on desired substrates at ease.
- (ii) Thickness of the desired thin film can be controlled to an acceptable extent.
- (iii) Evaporation of solvents is aided with airflow due to the rotation of the turntable/substrate.

Disadvantages

- (iv) High material wastage—up to 98% of the deposited precursor is flung off during the coating process, and only 2% is left on the substrate (Sahu et al. 2009). This makes spin coating relatively more expensive than other coating techniques where there is less material wastage.
- (v) Spin coating is not compatible with roll-to-roll production lines. This limits its use to lab-scale

experiments and prevents spin coating from making the transition into commercial applications. Substrate size is also limited to a small area, depending on the substrate holder.

b. Spin Coating in Perovskite Solar Cells.

Spin coating is widely used in perovskite solar cells' fabrication. It is used to deposit the electron transport layer (e.g., TiO₂) on FTO substrates, as well as the perovskite active layer and the hole transport layer (e.g., Spiro-OMeTAD) accordingly. The coating procedure is standard for all the layers with the addition of anti-solvent treatment for the perovskite active layer as discussed earlier.

5 Slot-Die Coating

Slot-die coating was invented by Beguin in 1954. The system comprised of a coating-die-head that passed a ribbon of the coating-material onto an adjacent strip-material (<https://patents.google.com/patent/US2681294A/en>). It is currently being used in various fields, such as batteries, for depositing the electrolyte slurry, optical coating, for anti-reflective coatings applied on windows and most recently, slot-die coating has been portrayed as the gateway between third-generation solar cells and commercialization (<https://www.ossila.com/pages/slot-die-coating-theory>). A modern lab-scale slot-die coater is shown in Fig. 14.

Slot-die coating has a great potential for the application in third-generation solar cells given that it is a pre-metered technique, where the thin-film thickness is dependent on the precursor/solution flow rate, it is also dependent on the slot-die-head's distance relative to the to be coated substrate, coating speed, heating temperature, which allows for a lot of room for optimization. Furthermore, slot-die coating is compatible with roll-to-roll (R2R) and sheet to sheet (S2S) production lines, where third-generation solar cells' precursors that make up electron transport materials (ETMs), hole transport materials (HTMs), and perovskite active layers, in liquid form, can be deposited on rolled or sheet flexible substrates making scaling up third-generation solar cells achievable in the near future.

5.1 Device Components

There are 3 main parts that a conventional slot-die coater consists of.

1. The slot-die-head, which is responsible for the direct precursor distribution upon substrates, has various design



Fig. 14 Slot-die coater

parameters that can be optimized according to the coating application.

2. The pumping (metering) system, which is responsible for the transfer of precursors to the head and supplies a constant or a varying flow rate.
3. The coating stage, which is where substrates are placed, determines the coating speed by how fast the stage is moving, using stepper motors, relative to the head or vice versa in some designs. A slot-die coater's stage can also utilize an integrated heater that meets the requirements of some applications.

5.2 Slot-Die-Head

A conventional slot-die-head, shown in Fig. 15, consists of an inlet, manifold, lands, and lips. Moreover, accessories such as shims and meniscus guides can be utilized to optimize and adjust the overall coating process.

1. When the precursor enters the slot-die-head through a metering system (e.g., a syringe pump), the first thing it faces is the inlet hole.
2. Then, the precursor starts to fill the manifold that is usually placed directly beneath the inlet, which then spills the precursor out to the land and slot of the

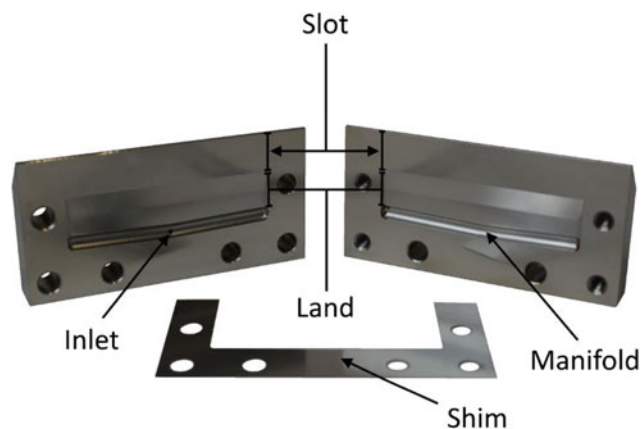


Fig. 15 Slot-die coating head (<https://www.ossila.com/pages/slot-die-coating-theory>)

die-head subsequently in order to start the coating process.

There are various designs of a slot-die-head's manifold that heavily influence the coating process. These designs are totally dependent on the difference in distances between the inlet and the exit of the die-head, and the manifold's lowest point and the exit of the die-head, such as shown in Fig. 16.

1. The T shaped manifold, shown in Fig. 16, presents an equal distance from the inlet and the edge of the manifold to the die-head exit. This results in a pressure difference moving away from the inlet and a variable (lower) flow rate near the edge of the manifold, as well as an uneven spread of the solution across the die-head and consequently the substrate (<https://www.ossila.com/pages/slot-die-coating-theory>).
2. Overcoming the issue of uniformity of the flow across the die-head exit, a coathanger manifold, shown in Fig. 16, can be utilized. The coathanger manifold reduces the distance from the manifold edge to the die-head exit while moving away from the inlet, which results in a uniform flow of the precursor across the width of the die-head exit. However, this design is dependent on the viscosity of the precursor that is being coated, and must be optimized accordingly, e.g., using shims to increase the width of the die-head channel (<https://www.ossila.com/pages/slot-die-coating-theory>).
3. To operate independently from the viscosity of the precursor, a constant shear manifold shown in Fig. 16 can be used. It varies the distance from the manifold edge to the exit of the die-head in a non-linear fashion, which in turn ensures a constant flow from the manifold edge to the die-head exit (<https://www.ossila.com/pages/slot-die-coating-theory>).

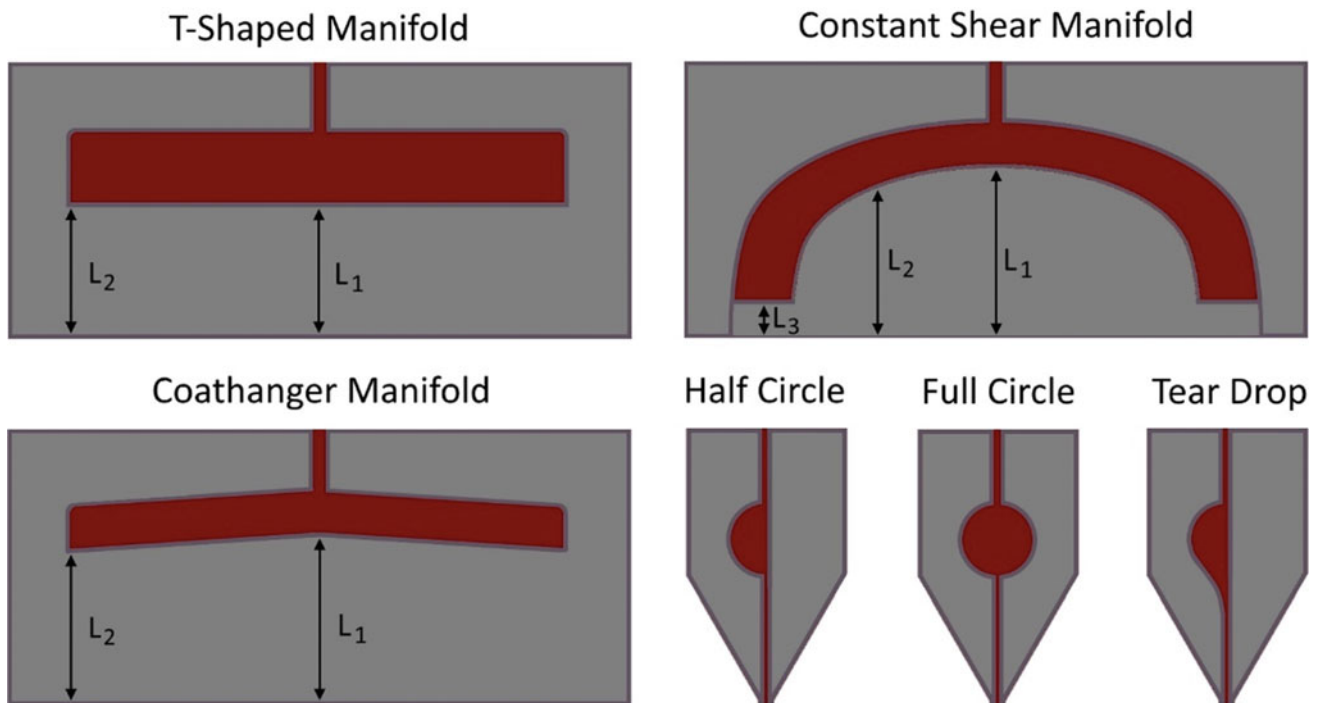
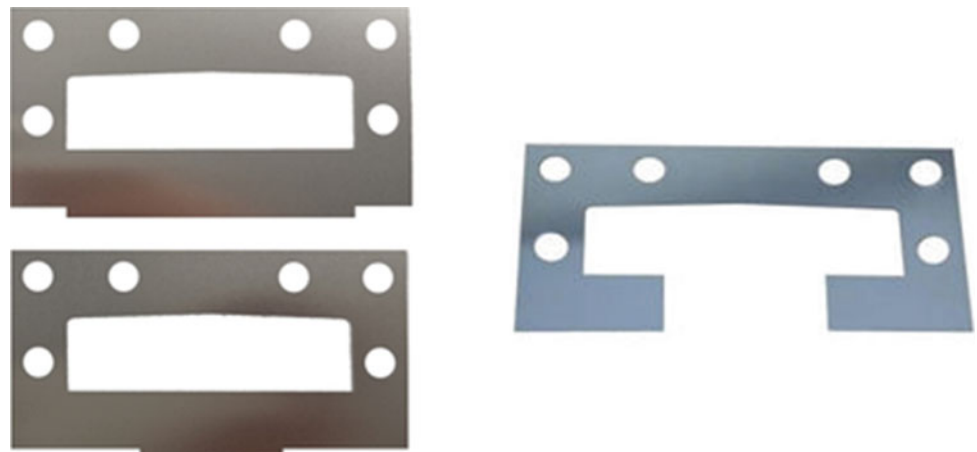


Fig. 16 Various manifold designs (<https://www.ossila.com/pages/slot-die-coating-theory>)

Fig. 17 Meniscus guide shim (https://www.ossila.com/products/slot-die-head?_pos=1&_sid=bc1331a13&_ss=r&variant=41159008878755)



For more info on head designs, the reader is encouraged to visit Ossila Website at: <https://www.ossila.com/pages/slot-die-coating-theory>.

Shims and meniscus guides can be used to have better control over the coating process in a slot-die coater as shown in Fig. 17. Depending on the design and number of shims used to adjust the width of the die-head channel, the die-outlet velocity can be directly controlled (Shin et al. 2020; Han et al. 2014).

Meniscus guides can also be implemented in order to control and direct the meniscus (point of contact between the die-head and the substrate) formation outside the die-head

and to adjust the relative distance from the die-head to the substrate (Krebs 2009), given that it extends out of the die-head lip.

5.3 Metering System

5.3.1 Syringe Pump

A syringe pump, shown in Fig. 18, is a lab-scale metering subsystem in slot-die coaters. It consists of a motor, pushing block, and a syringe. A precise motor moves the pushing block across a railway against the plunger flange of a syringe



Fig. 18 Syringe pump (<https://www.ossila.com/products/syringe-pump>)

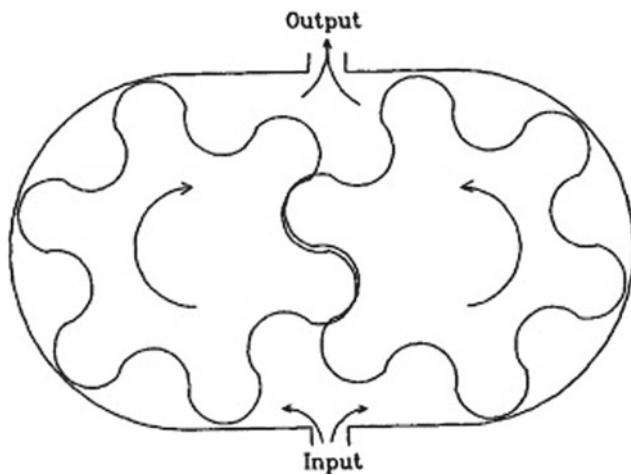


Fig. 19 Rotary pump with a gear and lobe design (Bajpai 2018) (with permission 5262570110935)

that can displace tiny volumes of the precursor into the slot-die-head with flow rates in the range of micro-liters per second. Lab-syringe pumps provide the option for complex programs of stepping up/down dispense rates depending on the application/experiment.

5.3.2 Rotary Pumps

A rotary pump (design shown in Fig. 19) is used for large-scale applications in slot-die coating. A liquid/precursor enters the rotary pump from one side and fills the passages of the gears, thus displacing them. As the gears are rotating, they pump the fluid/precursor away in the direction of the output of the pump. They are suited for viscous fluids, however, highly-viscous fluids require bigger pumps with low rotating speeds (Bajpai 2018).

5.4 Coating Principle

Slot-die coating is based on the delivery of liquids through the slot of the die-head and the deposition onto moving substrates by filling the gap between them. The boundaries of the die-head-substrate-gap are defined by upstream and downstream menisci that form what is known as the coating bead (Ding et al. 2016), such as shown in Fig. 20. The operation of slot-die coating is limited by the coating speed, liquid dispense rate, die-head-substrate gap, and liquid viscosity. There are three models that define the operating limits of slot-die coating, which are competing forces that influence the coating bead (<https://www.thefreelibrary.com/Comparison+of+vertical+and+horizontal+slot+die+coatings-a0171141698>; Romero et al. 2006).

1. Capillary model
2. Viscous model
3. Viscocapillary model

These models define what is known as the stable coating window, where any deviation away from it will cause defects in coated film. Defects such as chatter and ribbing, where the thickness of the coated film varies along the substrate with visible lines, uncontrollable dripping of the liquid, etc. (<https://www.ossila.com/pages/slot-die-coating-theory>).

5.4.1 Capillary Model

The coating stability in slot-die coating is totally dependent on the stability of the coating bead mentioned earlier. To ensure the stability of the coating bead, Beguin suggested the use of a vacuum box on the upstream meniscus (<https://patents.google.com/patent/US2681294A/en>). Ruschak (1976) set a model that defines limits for the vacuum pressure applied on the upstream meniscus based on capillary pressure on the coating bead with little regard to viscous effects, by using the inequalities shown in Eqs. (4) and (5).

$$-\frac{\sigma_u(1 + \cos \theta)}{h_u} + 1.34Ca^{\frac{2}{3}}\frac{\sigma_d}{t} \leq \Delta p \leq \frac{\sigma_u(1 - \cos \theta)}{h_u} + 1.34Ca^{\frac{2}{3}}\frac{\sigma_d}{t} \quad (4)$$

$$0 \leq \frac{1}{t} \leq \frac{1.49}{h_d} Ca^{-\frac{2}{3}} \quad (5)$$

where

σ : surface tension (upstream and downstream) of the menisci.

σ_d : represents the surface tension under atmospheric pressure.

Δp : vacuum pressure difference between the upstream and downstream menisci.

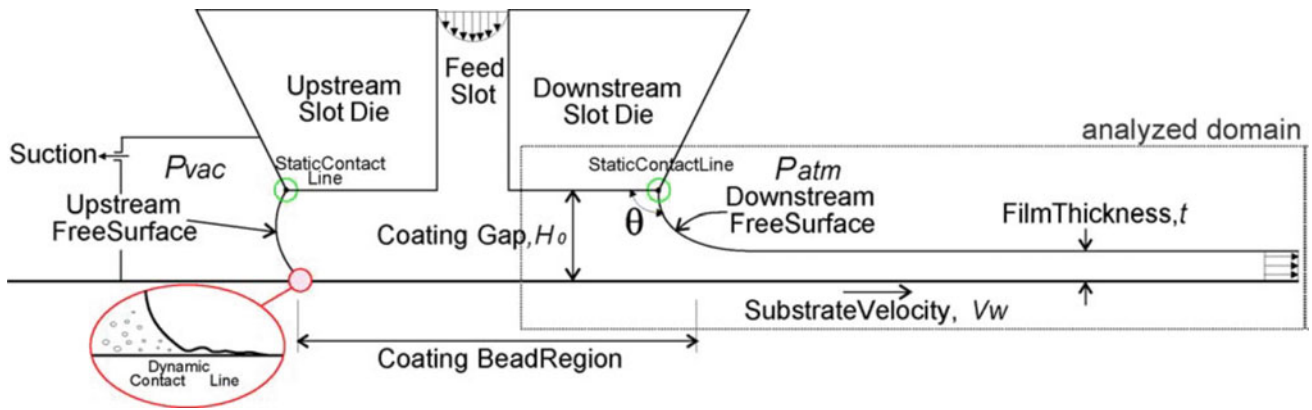


Fig. 20 Coating bead (Romero et al. 2006) (with permission 5262941365999)

Ca: capillary number (effect of viscous forces versus surface tension forces on the interface between a liquid and a gas).

h : coating gap.

θ : dynamic contact angle.

The upper and lower limits of the inequality shown in Eq. (4) represent the upper and lower limits of the vacuum pressure shown in Fig. 21. However, the line defining the upper limit does not cross the axis represented by $\frac{1}{l}$, which means that the thickness is infinitely large, making this model valid for thin coated films only (Ruschak 1976). The thin-film thickness when the pressure difference is zero is represented in Eq. (6).

$$t_0 = \frac{1.34\sigma_d}{\sigma_u} \text{Ca}^{\frac{2}{3}} \frac{h_u}{(1 + \cos \theta)} \quad (6)$$

As per Fig. 21, going below the coating window results in the upstream meniscus moving toward the exit of the die-head, leading to air entrapments and the formation of vortices this causes defects such as the ribbing and chattering

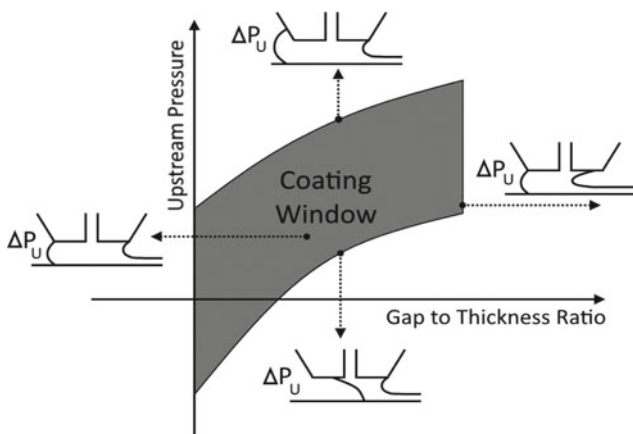


Fig. 21 Illustration of coating window with meniscus (<https://www.ossila.com/pages/slot-die-coating-theory>)

effects mentioned earlier (<https://www.ossila.com/pages/slot-die-coating-theory>).

Moving above and toward the upper limit of the coating window (usually due to the use of a vacuum box) causes the upstream meniscus to move past the upstream lip and to swell. This causes dripping and an uncontrollable variation in the thickness of the meniscus (<https://www.ossila.com/pages/slot-die-coating-theory>).

To the right of the coating window, the downstream meniscus starts to recede moving from left to right across the die-head, which causes air entrapments and the formation of bubbles that affect the end film (<https://www.ossila.com/pages/slot-die-coating-theory>).

5.4.2 Viscous Model

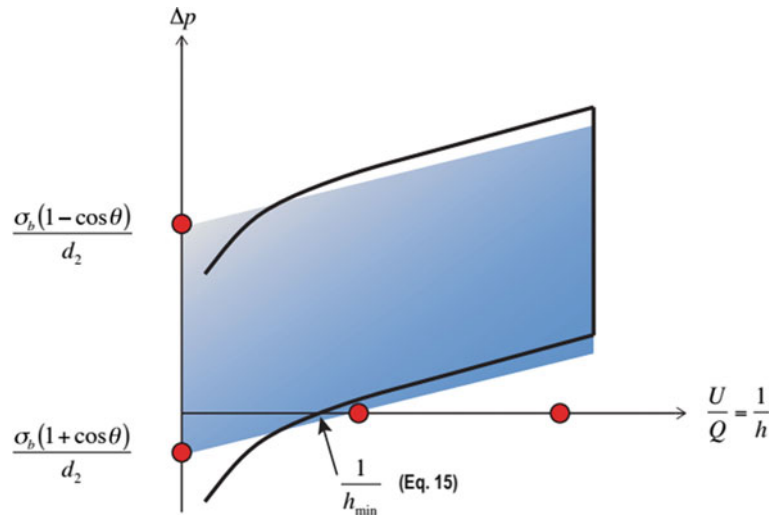
The operation in this model ignores capillary effects and takes into account viscous effects only on the coating bead (Higgins and Scriven 1980). In this model, the upstream meniscus is allowed to move across the upstream lip of the die-head, up until the downstream edge of the upstream lip, and variations in the coating speed or the vacuum pressure can lead to defects in the coated film (Ding et al. 2016). The stable coating window with respect to the vacuum pressure is defined in following inequality from Eq. (7). Where U is the coating speed and l is the lip length.

$$\frac{6\mu Ul_d}{h_d^2} \left[1 - \frac{2t}{h_d} \right] \leq \Delta p \leq \frac{6\mu Ul_d}{h_d^2} \left[1 + \frac{l_u h_d^2}{l_d h_u^2} - \frac{2t}{h_d} \right] \quad (7)$$

5.4.3 Viscocapillary Model

In the viscocapillary model, both capillary and viscous models are taken into account. Contrary to the viscous model, the upstream meniscus is not treated as pinned to the upstream edge of the die-head lip; however, it is treated as if it is free to move, which results in the following operating limits for the vacuum pressure provided in Eqs. (8) and (9) and illustrated in Fig. 22.

Fig. 22 Viscocapillary model stable coating window (Higgins 2011)



$$\Delta p \geq \frac{6\mu U l_d}{h_d^2} \left[1 - \frac{2t}{h_d} \right] - \frac{\sigma_u (\cos \theta_s + \cos \theta)}{h_u} + 1.34 \text{Ca}^{\frac{2}{3}} \frac{\sigma_d}{t} \quad (8)$$

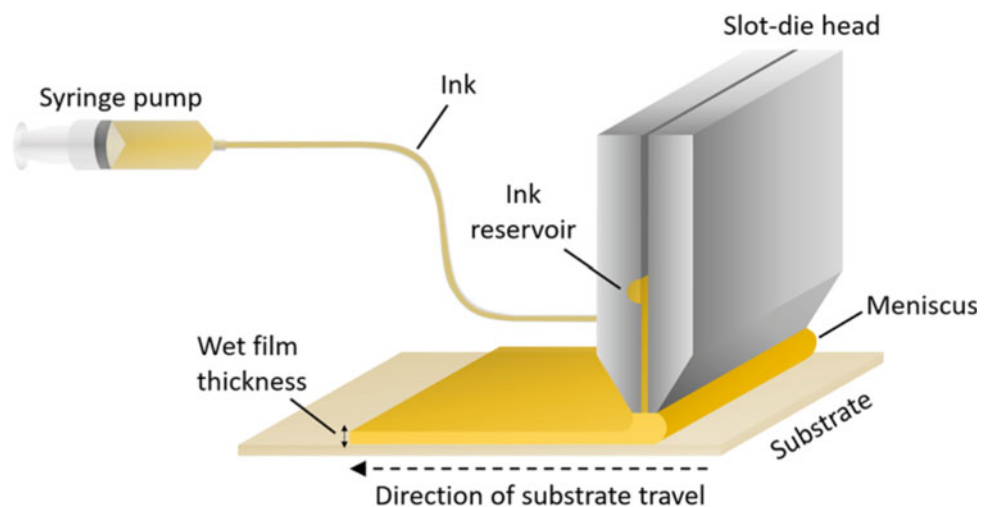
$$\Delta p \leq \frac{6\mu U l_d}{h_d^2} \left[1 + \frac{l_u h_d^2}{l_d h_u^2} - \frac{2t}{h_d} \right] - \frac{\sigma_u (\cos \theta_s + \cos \theta)}{h_u} + 1.34 \text{Ca}^{\frac{2}{3}} \frac{\sigma_d}{t} \quad (9)$$

5.5 Slot-Die Coating in Third-Generation Solar Cells

Slot-die coating is currently one of the most attractive techniques to fabricate third-generation solar cells (dye-sensitized solar cells and perovskite solar cells). This is

due to its capability to uniformly coat thin films across large areas, with throughput speeds reaching 600 m/min (Patidar et al. 2020) as well as the high compatibility with R2R (roll-to-roll) and S2S (sheet-to-sheet) production lines, such as shown in Fig. 23. Unlike spin coated perovskite/third-generation solar cells, the use of an anti-solvent is not an option. Post-treatments such as vacuum or nitrogen quenching are used to extract/remove the solvents from the wet film before it dries and crystalizes. For vacuum quenching, a coated perovskite sample is subject to a low level of vacuum pressure in vacuum chamber in order to extract away the solvents, most commonly dimethylformamide (DMF) and dimethyl sulfoxide (DMSO). Nitrogen quenching is used to assist with the evaporation of the previously mentioned solvents and to aid with the crystallization of the film (Du et al. 2020).

Fig. 23 Slot-die coating process (Patidar et al. 2020) (with permission 5263681213473)



6 Thermal Evaporation

Thermal evaporation is a physical vapor deposition technique that is used regularly in third-generation solar cells for depositing thin films that take on the transport of generated electron/hole pairs toward the solar cells' contacts, also known as electron/hole transport layers as well as gold/silver contacts. It uses resistive heating (joule heating) to evaporate a solid material, in powder or pallet form, onto a desired substrate in a vacuum environment. Thermal evaporation is suited for high rates of deposition, simple and considered to be of low cost. In this section, thermal evaporation device components and coating principle will be discussed.

6.1 Device Components

A thermal evaporator, such as shown in Fig. 24, consists of a



Fig. 24 Thermal evaporator

Fig. 25 Thermal evaporator glass chamber with protective mesh around it **a** open and **b** closeup



(a)

(b)

1. A glass chamber, such as shown in Fig. 25, which comes in a bell shape and ensures an isolated environment within it with the aid of rubber sealant gaskets.
2. A chamber elevator, highlighted in Fig. 24, is responsible for lifting and lowering the glass chamber during the beginning and the end of a coating process.
3. Resistive heaters/boat holder, such as shown in Fig. 26, which takes upon the task of raising the temperature of the boat that harbors the target/source material by passing an electrical current through it.
4. A substrate(s) holder, shown in Fig. 27, which is usually right above the boat/resistive heaters, is where the substrates are placed. A substrate holder is fixed on a rotating platform to ensure that all the substrates are equally exposed to the evaporated material. Substrates are secured onto the substrate holder using a heat resistant double tape.
5. Vacuum pump/nitrogen system is connected to the thermal evaporator chamber in order to achieve the desired vacuum environment required for a smooth evaporation/deposition process. See Fig. 25a for the vacuum pump in the lower left of Figure.
6. A control interface is used to lift or lower the glass chamber, trigger the rotation of the substrate holder, start the vacuum/vent process, and control the current flowing through the resistive heaters.

6.2 Thermal Evaporation Coating Steps

1. A source material is usually placed in a tungsten crucible (boat), and tungsten is most commonly used due to its high melting temperature of 3410 °C (<https://www.britannica.com/science/tungsten-chemical-element>).

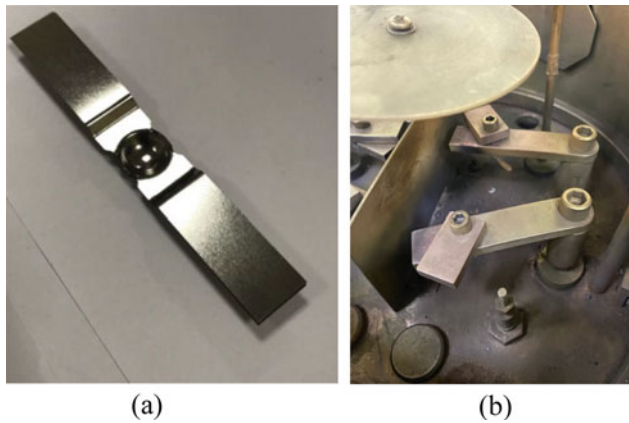


Fig. 26 a Boat/ resistive heaters, b location in thermal evaporator

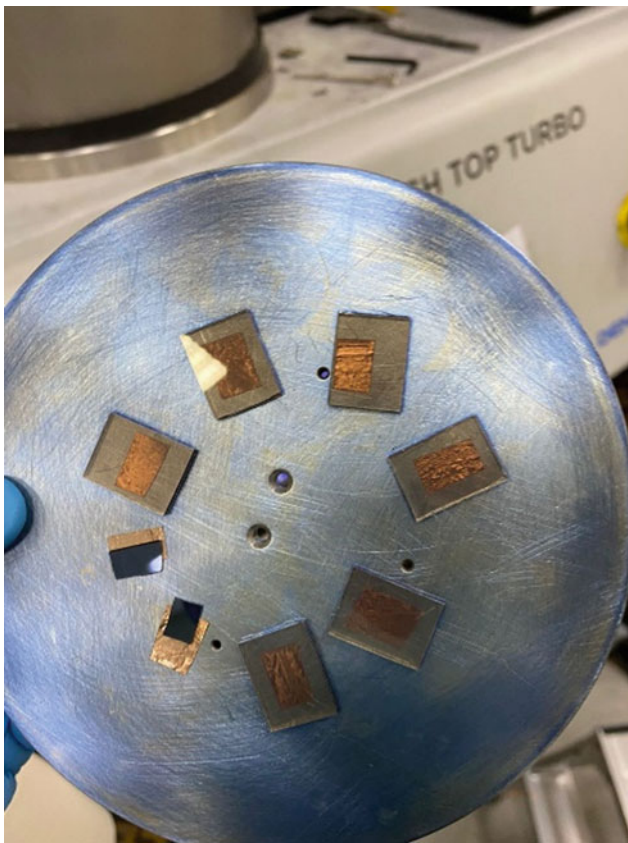


Fig. 27 Substrate holder

2. The targeted substrate, usually glass/conductive oxide coated glass or metal, is secured on a substrate holder above the boat.
3. A vacuum pump creates an inert environment for the evaporation to take place in, this step is crucial not to cause unnecessary oxidation of the deposited thin film (Lévy 2016).

4. After reaching a low enough vacuum pressure, around 10^{-2} Pa (Lévy 2016), the coating process can start.
5. Through a control interface, the current passing through the boat which results in heating it is stepped-up gradually up until the source material starts vaporizing—evaporation temperature is reached.
6. As the material is evaporating, it leaves the boat and ascends toward the substrate, and the inert condition removes the air-drag factor allowing for a smooth transition of the vapor from the boat to the desired substrate.
7. When the vapor reaches the relatively colder substrate, a phase change process takes place leading to a solidified thin film on the substrate.
8. Through the interface of the thermal evaporator, the evaporation rate can be always obtained. When a desired evaporation rate is reached, the current passing can be held constant unless there is a variation in the evaporation rate due to the lack of leftover source material.
9. When the thin film reaches a desired thickness, the current is stepped down gradually to protect the source material and the boat from fracture, and the thermal evaporator chamber is vented.
10. The substrate is then removed from the thermal evaporation chamber, and it can undergo any desired post-deposition treatment (i.e., annealing).

The overall coating process is shown in the schematic presented in Fig. 28.

7 Doctor Blade Coating

Doctor blade coating is a technique that has been utilized in the deposition of the perovskite active layer in perovskite solar cells and third-generation solar cells in general, such as shown in Fig. 29. The solution to be coated is placed in front of the blade, which is held at a set distance from the targeted substrate. The blade is then moved across the substrate, spreading the solution and resulting in a wet film with a desired thickness. The base operation of doctor blade coating deems it to be roll-to-roll compatible, allowing for its implementation in high throughput applications.

In terms of material wastage, doctor blade coating is said to have a solution loss of about 5% (Mishra et al. 2019) after an optimization process has taken place. In comparison with slot-die coating which is a similar roll-to-roll printing technique, doctor blade coating requires way less precursor solution to operate (Yilbas et al. 2019). Doctor blade-coated films' thicknesses are controlled by optimizing the concentration of the perovskite precursor (by adjusting the ratio and volume of the organic solvents that are used), blade speed, and the blade-substrate distance.

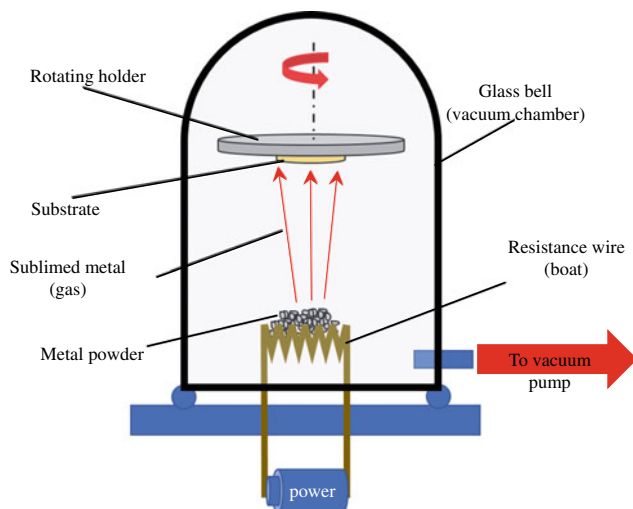


Fig. 28 Thermal evaporation coating process (with permission 5273140799497)

For a precursor to be compatible with doctor blade coating, it has to contain a relatively higher amount of binders and thickeners, in comparison with other roll-to-roll coating techniques, resulting in high viscosities ranging from 1000 to 10,000 mPa.s (Shin et al. 2020).

Perovskite solar cells were prepared by Wang et al. (Han et al. 2014), using doctor blade coating for the perovskite active layer and nickel oxide (NiO) as a hole transporting material instead of the conventional organic PEDOT:PSS. They achieved a 200 μm crystal domain for the perovskite active layer and a power conversion efficiency of 15.34%.

8 Curtain Coating

Curtain coating is a pre-metered coating technique that creates a continuous curtain of a flowing fluid which falls onto a moving substrate. This technique utilizes a tank that harbors the ink/precursor to be coated, with a slit or a slot-die-head to facilitate the fluid delivery, and a conveyer

belt to move the substrate across the curtain of fluid (<https://www.ossila.com/pages/slot-die-coating-theory>), a conventional curtain coating process is shown in Fig. 30.

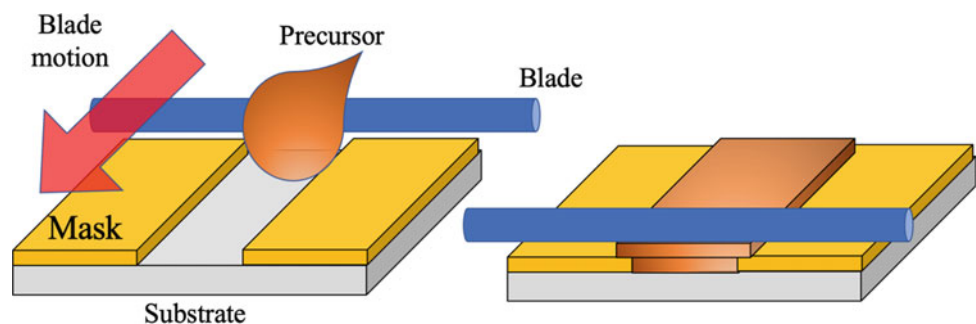
Third-generation solar cell precursors can be prepared and fed into a tank suited for curtain coating, with all the material property requirements taken into account, for direct roll-to-roll fabrication of these novel technologies. Precursor properties are essential to consider given that curtain coating operational variables depend on a base parameter known as the minimum flow rate for each liquid/precursor that can be used for a successful coating process. The minimum flow rate is a function of surface tension and the viscosity (in the range of 10–500 mPa.s (Ruschak 1976)) of the precursor used.

Curtain coating being a pre-metered techniques means that the amount of material that is used to achieve a certain thickness of the deposited material can be calculated beforehand. The flow rate of the fluid curtain is set with respect to the volume of the tank and the amount of material that is available, and the speed of the conveyer belt with respect to the width of the cell can be used to calculate exactly the amount of material that is deposited on the substrate within a single coating process. This allows for a moderately precise thickness control with little to no material waste (Higgins and Scriven 1980), and in case, there is excess material that was not utilized in the coating process, and a retrieving pan/bowl is placed beneath the conveyer belt as a collection station that pumps back the unused fluid into the holding tank (Krebs et al. 2009).

9 Pad Printing

Pad printing is a gravure offset printing technique that has a high throughput and a simple design. Pad printing consists of a flexible silicon rubber pad, a printing cliché (etched printing plate) that has the desired to be printed design engraved on it, and a doctor blade for spreading the ink across the cliché.

Fig. 29 Doctor blade coating process



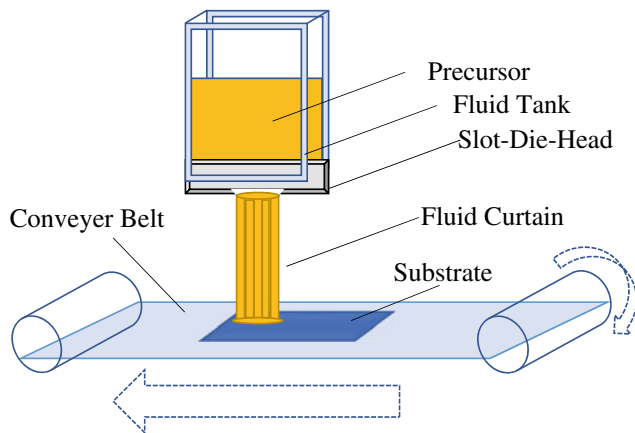


Fig. 30 Curtain coating process

The first step of pad printing is transferring the ink onto the cliché via a spatula and doctor blading the excess material away, while filling the engraved design with the desired ink. The volatile solvents start evaporating from the ink at this stage.

Then, the flexible silicon rubber pad is lowered to reach the cliché and picks up the ink as well as some of the leftover solvents. As the ink sticks onto the pad, the rest of the solvents still imbedded within the ink are evaporated. The pad is then lowered to come in contact with a non-planar solar cell surface (porous surface) and transfers the ink during the process. A conventional pad printing process is shown in Fig. 31.

To counter the issue of rapid evaporation of the conventional inks that are used in other techniques such as screen printing, an optimization of the ink precursors must take place by adjusting the type and ratio of the binders and solvents used.

The shape of the silicon pad also affects the overall printing process. Parameters that decide the curvature of the

pad are the shape and roughness of the substrate that the printing is set to take place onto.

Pad printing is compatible with roll-to-roll production lines to some extent and has a very high material utilization with little to no wastage and a moderate thickness control that is affected by the ink that is used and the solvents involved, as well as intermediate ink viscosity requirements of 10–200 mPa.s (Ruschak 1976).

10 Spray Coating

Spray coating is a primary process in surface engineering applications, such as wear and corrosion prevention. It is a cost-effective solution that has been implemented in a variety of industries given that it is compatible with roll-to-roll production lines.

The process of spray coating begins with the material feedstock which is molten or semi-molten powder. Through the spray coating-nozzle's barrel, the material is propelled onto the desired substrate through a stream of hot gas or plasma. Temperature control mechanisms are used to ensure that the targeted substrate is kept at a temperature that suits the coating material. Once the coating material reaches the cool surface of the substrate, it cools down and subsequently contracts forming a very strong bond with the substrate's surface. The coating is done layer by layer to reach a desired thickness. However, the thickness is not precisely controlled in this process in comparison with other roll-to-roll alternatives. Spray coating process is illustrated in Fig. 32.

Spray coating has an adverse high material wastage, given that the base of the coating process does not allow for a precise ejection of the source material. Spray coating requires a relatively low viscosity of the molten source material at 1–40 mPa.s (Ruschak 1976).

Fig. 31 Pad printing process

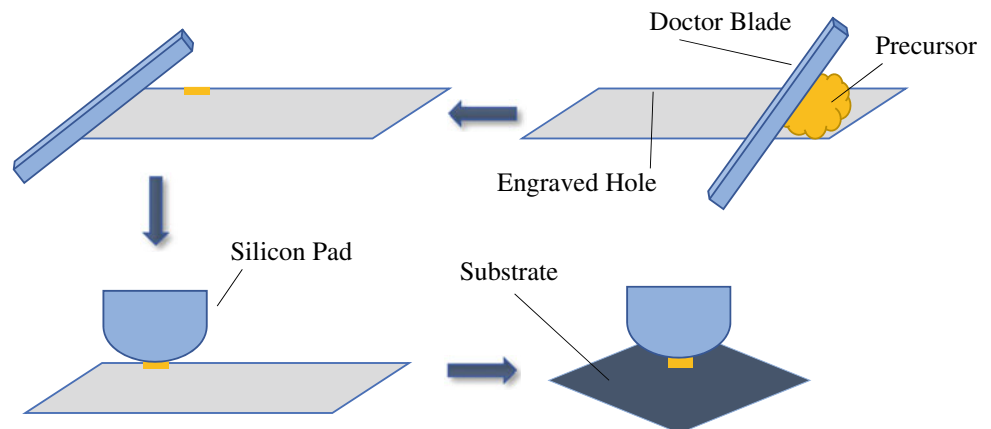
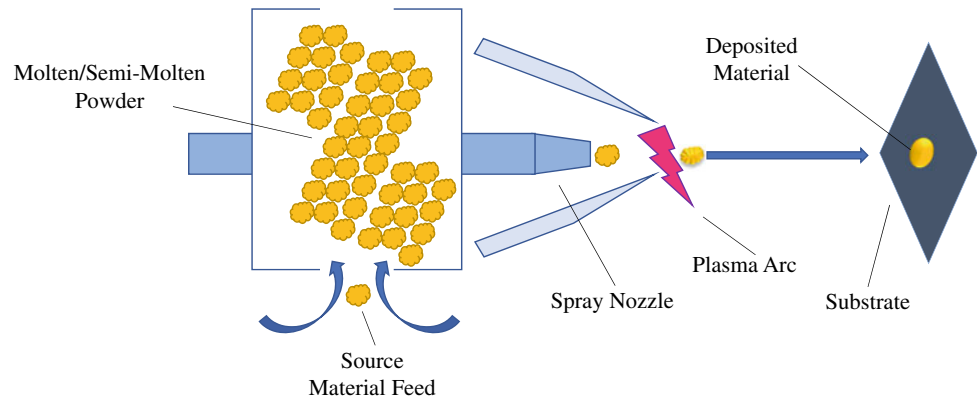
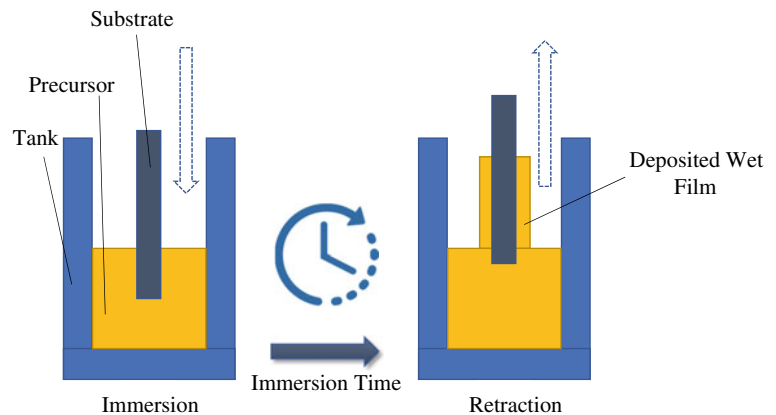


Fig. 32 Spray coating process**Fig. 33** Dip coating process

11 Dip Coating

Dip coating is an established industrial process that is compatible with various kinds of substrates, including those of conventional third-generation solar cells. Dip coating is relatively simpler than comparable roll-to-roll systems. It essentially consists of a precursor-containing tank, and a substrate that can be immersed into or rolled in and out of the tank. The layer that is deposited on the substrate depends on the immersion time, surface tension, and the viscosity (1–200 mPa.s (Ruschak 1976)) of the solution/precursor.

Dip coating is considered to be one of the most effective techniques of fabricating perovskite solar cells, with low cost and a precisely controllable layer thickness with few drawbacks such as a relatively slow production rate (Vak et al. 2015).

The dip coating process, such as shown in Fig. 33, consists of two steps. A targeted substrate is immersed into a precursor-containing tank with optimized precursor properties, and the immersion speed is controlled through an immersing hand. A sufficient immersion time is spent to allow the precursor to stick to the substrate resulting in a workable wet film. The second step is retracting the substrate

at a speed that suits the surface tension and the viscosity of the precursor and moving it along the production line for further processing.

References

- Bajpai P (2018) Hydraulics. In: Biermann's handbook of pulp and paper. Elsevier, pp 455–482. <https://doi.org/10.1016/B978-0-12-814238-7.00023-4>
- Burgelman M (1998) Thin film solar cells by screen printing technology
- Chemical Resistance Guide of PTFE and Filled PTFE [Online]. Available: <http://www.standard-ptfe.com/chemical-resistance-guide-of-ptfe-and-filled-ptfe.php>
- Coaters LS, Spin coaters from Laurell—WS-650–23B spin coater. Laurell Technologies Corporation [Online]. Available: <http://www.laurell.com/spin-coater/?model=WS-650-23B&s=2>
- Comparison of Vertical and Horizontal Slot Die Coatings. Free Online Library. <https://www.thefreelibrary.com/Comparison-of-vertical-and-horizontal-slot-die-coatings-a0171141698> (accessed Jul. 20, 2022)
- Ding X, Liu J, Harris TAL (2016) A review of the operating limits in slot die coating processes. *AIChE J* 62(7):2508–2524. <https://doi.org/10.1002/aic.15268>
- Du M et al (2020) High-pressure nitrogen-extraction and effective passivation to attain highest large-area perovskite solar module

- efficiency. *Adv Mater* 32(47):2004979. <https://doi.org/10.1002/adma.202004979>
- Guo G et al (2011) Effect of dispersibility of silver powders in conductive paste on microstructure of screen-printed front contacts and electrical performance of crystalline silicon solar cells. *J Mater Sci: Mater Electron* 22(5):527–530. <https://doi.org/10.1007/s10854-010-0172-1>
- Han GH, Lee SH, Ahn W-G, Nam J, Jung HW (2014) Effect of shim configuration on flow dynamics and operability windows in stripe slot coating process. *J Coat Technol Res* 11(1):19–29. <https://doi.org/10.1007/s11998-013-9485-3>
- Higgins B (2011) Slot die coating: the physics of the viscocapillary coating bead. https://www.researchgate.net/publication/245320474_Slot_Die_Coating_The_Physics_of_the_Viscocapillary_Coating_Bead (accessed Jul. 24, 2022)
- Higgins BG, Scriven LE (1980) Capillary pressure and viscous pressure drop set bounds on coating bead operability. *Chem Eng Sci* 35(3):673–682. [https://doi.org/10.1016/0009-2509\(80\)80018-2](https://doi.org/10.1016/0009-2509(80)80018-2)
- Hussain W, Rashid B, Sridewi N, Ahmed W, Ahmad MS (2022) Development of dye-sensitized solar cell module and its optimization. In: *Dye-sensitized solar cells*. Elsevier, pp 137–157. <https://doi.org/10.1016/B978-0-12-818206-2.00009-8>
- Krebs FC (2009) Polymer solar cell modules prepared using roll-to-roll methods: knife-over-edge coating, slot-die coating and screen printing. *Sol Energy Mater Sol Cells* 93(4):465–475. <https://doi.org/10.1016/j.solmat.2008.12.012>
- Krebs FC, Gevorgyan SA, Alstrup J (2009) A roll-to-roll process to flexible polymer solar cells: model studies, manufacture and operational stability studies. *J Mater Chem* 19(30):5442. <https://doi.org/10.1039/b823001c>
- Lévy F (2016) Film growth and epitaxy: methods. In: *Reference module in materials science and materials engineering*. Elsevier, B9780128035818010000. <https://doi.org/10.1016/B978-0-12-803581-8.01012-2>
- Mishra A, Bhatt N, Bajpai AK (2019) Chapter 12—Nanostructured superhydrophobic coatings for solar panel applications. In: Nguyen Tri P, Rtimi S, Plamondon CMO (eds) *Nanomaterials-based coatings*. Elsevier, pp 397–424. <https://doi.org/10.1016/B978-0-12-815884-5.00012-0>
- Newport M (2022) Semiconductor lithography. <https://www.newport.com/n/photolithography-overview>
- Orava J, Kohoutek T, Wagner T (2014) Deposition techniques for chalcogenide thin films. In: *Chalcogenide glasses*. Elsevier, pp 265–309. <https://doi.org/10.1533/9780857093561.1.265>
- Patidar R, Burkitt D, Hooper K, Richards D, Watson T (2020) Slot-die coating of perovskite solar cells: an overview. *Mater Today Commun* 22:100808. <https://doi.org/10.1016/j.mtcomm.2019.100808>
- PP Polypropylene Natural Specifications Boedeker [Online]. Available: <https://www.boedeker.com/Product/Polypropylene-Natural>
- Ramasamy E, Lee WJ, Lee DY, Song JS (2007) Portable, parallel grid dye-sensitized solar cell module prepared by screen printing. *J Power Sources* 165(1):446–449. <https://doi.org/10.1016/j.jpowsour.2006.11.057>
- Romero OJ, Scriven LE, Carvalho MS (2006) Slot coating of mildly viscoelastic liquids. *J Nonnewton Fluid Mech* 138(2–3):63–75. <https://doi.org/10.1016/j.jnnfm.2005.11.010>
- Ruschak KJ (1976) Limiting flow in a pre-metered coating device. *Chem Eng Sci* 31(11):1057–1060. [https://doi.org/10.1016/0009-2509\(76\)87026-1](https://doi.org/10.1016/0009-2509(76)87026-1)
- Sahu N, Parija B, Panigrahi S (2009) Fundamental understanding and modeling of spin coating process: a review. *Indian J Phys* 83(4):493–502. <https://doi.org/10.1007/s12648-009-0009-z>
- Saraie J, Kitagawa M, Ishida M, Tanaka T (1978) Liquid phase epitaxial growth of CdTe in the CdTe–CdCl₂ system
- Shin D, Lee J, Park J (2020) Effect of slit channel width of a Shim embedded in slot-die-head on high-density stripe coating for OLEDs. *Coatings* 10(8):772. <https://doi.org/10.3390/coatings10080772>
- Solution Processed Metal Oxide Thin Films for Electronic Applications (2020) Elsevier. <https://doi.org/10.1016/C2017-0-02104-3>
- Slot-Die Coating Theory, Design & Applications | Ossila. <https://www.ossila.com/pages/slot-die-coating-theory> (accessed Jul. 20, 2022)
- Slot-Die Coating Theory, Design & Applications | Ossila. <https://www.ossila.com/pages/slot-die-coating-theory> (accessed Feb. 15, 2023)
- Slot-Die Head, Shims & Meniscus Guides | Coater Accessories | Ossila. https://www.ossila.com/products/slot-die-head?_pos=1&_sid=bc1331a13&_ss=r&variant=41159008878755 (accessed Jul. 24, 2022)
- Spin Coater Low Price Compact Spin Coating System. *Ossila* [Online]. Available: <https://www.ossila.com/products/spin-coater>
- Spin Coating: Complete Guide to Theory and Techniques. *Ossila* [Online]. Available: <https://www.ossila.com/pages/spin-coating>
- Spincoating SPSE, POLOS300 advanced. www.spincoating.com [Online]. Available: <https://www.spincoating.com/en/spin-coater-models/spincoater-polos300-advanced-spin-coating-machine/28/>
- Syringe Pump | Low Price Single/Dual Laboratory Device | Ossila. <https://www.ossila.com/products/syringe-pump> (accessed Jul. 24, 2022)
- Summers H (ed) (2013) vol 5. Elsevier, Amsterdam; Boston
- Teixeira ES et al (2020) Building and testing a spin coater for the deposition of thin films on DSSCs. *Mat Res* 23(6):e20200214. <https://doi.org/10.1590/1980-5373-mr-2020-0214>
- Thin Film Solar Cells by Screen Printing Technology | Semantic Scholar. <https://www.semanticscholar.org/paper/Thin-film-solar-cells-by-screen-printing-technology-Burgelman/f7a356e1c66f443a5604c07d69dbfc0de714cc77> (accessed Jul. 20, 2022)
- tungsten Uses, Properties, & Facts Britannica [Online]. Available: <https://www.britannica.com/science/tungsten-chemical-element>
- US2681294A—Method of Coating Strip Material—Google Patents. <https://patents.google.com/patent/US2681294A/en> (accessed Jul. 20, 2022)
- Vak D et al (2015) 3D printer based slot-die coater as a lab-to-fab translation tool for solution-processed solar cells. *Adv Energy Mater* 5(4):1401539. <https://doi.org/10.1002/aenm.201401539>
- Yilbas BS, Al-Sharafi A, Ali H (2019) Chapter 3—Surfaces for self-cleaning. In: Yilbas BS, Al-Sharafi A, Ali H (eds) *Self-cleaning of surfaces and water droplet mobility*. Elsevier, pp 45–98. <https://doi.org/10.1016/B978-0-12-814776-4.00003-3>